**Annales
Geophysicae**

Wavelet transforms of meteorological parameters and gravity waves

Z. Can[1], Z. Aslan[2], O. Oguz[2], and A. H. Siddiqi[3]

[1]Yildiz Technical University, Faculty of Science and Letters, Dept. of Physics, Istanbul, Turkey
[2]Faculty of Engineering and Design, Istanbul Commerce University, Istanbul, Turkey
[3]King Fahd University of Petroleum and Minerals, Department of Mathematical Sciences, Dhahran, Saudi Arabia

Abstract. The main purpose of this paper is to analyze some
characteristics of gravity waves (GWs), and seasonal varia-
tions of atmospheric waves over Istanbul by using wavelet
techniques. Daily radiosonda data of Istanbul in the tro-
posphere and lower stratosphere (1000 hPa–30 hPa) between
1993 and 1997 have been considered. Wavelet analysis based
on a computer simulation of data is generally close to the
real data when Daubechies wavelet series are used. Daily,
monthly, seasonal and annual variations of pressure heights,
air temperature and deviations from mean values have been
analyzed. Variations show the effects of gravity waves for
different pressure levels in the troposphere. These waves
lead to the meso-scale wave-form structures in spring, au-
tumn and winter. As a result of this study, wavelet series
and transforms for data construction, definition of some discon-
tinuities and the local effects on the signal have been compared
with the results of previous studies. The most similar struc-
ture between temperature, turbulence parameters and geo-
potential height deviations has been defined at the 500-hPa
pressure level.

Keywords. Atmospheric composition and structure (pres-
sure, density and temperature) – Meteorology and atmo-
spheric dynamics (convective processes; turbulence)

1 Introduction

Dynamics and thermodynamics of the lower atmosphere de-
termine its physical conditions. Wind, temperature and hu-
midity profiles have a crucial role in the growing and propa-
gation of turbulence and internal gravity waves. Many exper-
imental campaigns have been carried out to study the charac-
teristics and effects of gravity waves in the lower, middle and
upper atmosphere over the last decades (Isaac et al., 2004).

The wavelet transform was applied to the analysis of
characteristics of thermal and velocity fields of coherent

structures from turbulence data taken within and above a de-
ciduous forest by Gao and Li (1993). This study demon-
strates the usefulness of wavelet analysis in decomposing
structures at different scales, hidden in time series data. The
wavelet technique is a useful tool for analyzing time series
with many different time scales or changes in variance. A
practical step-by-step guide to wavelet analysis is given with
examples taken from time series of the El Niño-Southern Os-
cillation (ENSO) (Torrence and Compo, 1998).

Wavelet methods have been applied to the study of the sta-
ble atmospheric boundary layer under non-stationary condi-
tions by Terradellas et al. (2001). Wavelet analysis is a useful
tool to determine the dominant modes of the signal, as well
as its evolution in time. It also provides easier detection of
short duration events in large series.

Zink and Vincent (2001) described a technique to detect
gravity wave packets in high-resolution radiosonde sound-
ings of horizontal wind and temperature. A strong seasonal
cycle in the total wave variance was found with a maximum
in winter.

A calendar of the negative and positive phases of the North
Sea-Caspian Pattern (NCP) for the period 1958–1998 was
used to analyze the implication of the NCP upper level tele-
connections on the regional climate of the eastern Mediter-
ranean basin (Kutiel et al., 2002). The maximum impact of
the NCP on mean air temperature was detected in the con-
tinental Anatolian Plateau, where the mean seasonal differ-
ences are around 3.5°C. This influence decreases westwards
and southwards.

A sudden temperature rise in the lower thermosphere can
support surface waves propagating horizontally with energy
concentrated near the sudden temperature rise (Ding et al.,
2003). The energy distribution is shifted toward the lower at-
mosphere when compared with wave modes without winds.
The descent of energy distribution makes the energy atten-
uation caused by viscosity and thermal conductivity drops
down. This leads to the rise of attenuation distances.

The purpose of the present study is to understand the
characteristics of lower atmospheric turbulent structure and

Table 1. Seasonal average values of pressure height deviations between 1000 and 300 hPa pressure levels.

300 hPa(dh)	spring	summer	autumn	winter	annual
1993	125.86	95.04	115.76	115.37	124.30
1994	120.76	79.67	64.57	105.08	99.72
1995	130.42	58.27	136.63	172.43	78.49
1996	119.6	76.32	121.79	169.92	105.13
1997	129.79	84.60	106.32	90.82	133.62
mean	125.29	78.78	109.01	130.72	108.25
500 hPa(dh)					
1993	87.81	57.75	70.05	79.27	84.76
1994	80.05	53.15	42.37	73.13	66.93
1995	80.76	35.37	85.48	66.22	70.78
1996	79.73	51.75	76.73	66.54	69.62
1997	91.69	51.88	72.72	55.51	87.11
mean	84.01	49.98	69.47	68.13	75.84
700 hPa(dh)					
1993	60.26	32.57	45.06	54.63	58.99
1994	54.03	40.10	28.46	54.09	47.60
1995	47.19	25.54	49.91	46.93	45.10
1996	54.20	33.41	50.40	44.8	47.53
1997	56.87	53.84	46.90	41.63	51.69
mean	54.51	37.09	44.15	48.42	50.18
850 hPa(dh)					
1993	48.93	25.77	32.42	46.16	42.38
1994	38.56	30.20	37.31	50.58	40.09
1995	36.89	23.70	41.83	50.52	40.60
1996	44.22	25.31	39.61	43.88	40.81
1997	47.11	28.5	38.70	48.65	39.72
mean	43.14	26.70	37.97	47.96	40.72
1000 hPa(dh)					
1993	40.28	29.72	43.53	44.78	43.10
1994	35.62	27.65	30.44	56.37	34.86
1995	38.13	26.11	42.27	61.21	44.75
1996	38.93	28.20	39.46	53.90	42.47
1997	49.37	30.68	43.39	67.25	45.99
mean	40.47	28.47	39.82	56.70	42.23

Table 2. Seasonal average values of temperature deviations between 1000 and 300 hPa pressure levels.

300 hPa (dT)	spring	summer	autumn	winter	annual
1993	5.69	3.54	2.93	3.07	4.07
1994	3.04	2.87	4.77	2.07	3.36
1995	3.16	2.33	3.14	2.91	2.75
1996	2.76	3.49	3.70	3.17	3.20
1997	3.08	3.06	2.82	2.15	3.06
mean	3.55	3.06	3.47	2.67	3.29
500 hPa (dT)					
1993	3.38	2.76	3.23	3.34	3.59
1994	3.34	2.08	1.96	3.18	2.68
1995	4.18	1.78	4.92	4.80	3.91
1996	3.44	3.07	3.44	3.08	3.76
1997	4.20	2.73	3.15	3.06	3.36
mean	3.71	2.48	3.34	3.49	3.46
700 hPa (dT)					
1993	3.58	3.46	4.32	3.63	4.24
1994	3.87	2.79	2.65	4.00	3.24
1995	4.45	1.98	4.58	3.80	3.91
1996	4.25	3.12	3.65	4.00	3.85
1997	4.76	3.15	3.40	3.52	3.91
mean	4.18	2.9	3.72	3.79	3.83
850 hPa (dT)					
1993	4.66	3.98	5.71	3.83	4.91
1994	5.28	3.30	3.60	4.64	4.20
1995	4.96	2.07	4.52	4.57	4.26
1996	4.41	3.58	3.77	4.72	4.05
1997	4.70	4.55	4.37	4.86	4.61
mean	4.8	3.5	4.39	4.52	4.41
1000 hPa (dT)					
1993	4.16	2.33	3.99	3.62	3.55
1994	4.43	1.99	2.39	4.09	3.31
1995	3.73	1.14	3.06	3.91	3.24
1996	2.90	1.96	3.14	3.86	3.09
1997	4.39	2.62	3.05	4.03	3.62
mean	3.92	2.01	3.13	3.90	3.36

internal gravity waves in the vicinity of Istanbul. The main objectives of this paper are listed below:

1. To define the variation of gravity wave characteristics in a time domain.

2. To apply 1-D-wavelet analysis and wavelet packets and to explain discontinuities in the daily variations of air temperature, pressure heights, thermal conductivity and viscosity.

3. To analyze seasonal variations of gravity waves by considering radiosonda data and to compare the results with the large-scale effects such as La-Niña and El-Niño.

2 Material and methodology

2.1 Description of study area and data

The air temperature and pressure height observations using the radiosonda sounding system at 00:00 GMT, between 1993 and 1997 at Goztepe (Istanbul: $40°55'$ N, $29°05'$ E), have been analyzed. The study area (Göztepe Observatory) is at the transient region of two continents: Europe and Asia. It is under the effects of land-air-sea interactions. This contrast and temperature differences trigger a thermal turbulent structure of the atmospheric boundary layer.

Time variation of daily pressure height and standard deviations of air temperature and pressure heights up to the 300-hPa pressure level have been analyzed in this paper. Standard deviations have been presented in the following sections.

2.2 Tools and methodology

MATLAB and SPSS packet programs were used as a tool for the main objectives of this study (Aslan and Oguz, 1998; Aslan et al., 1997; Can et al., 2002).

2.3 Continuous 1-D-wavelet

The wavelet analysis is a great improvement in the analysis of atmospheric data, especially in studying the displacement characteristics of a moving structure (Meyer, 2000; Terradellas et al., 2001) . The guide includes a comperative study of the windowed Fourier transform, the choice of an appropriate wavelet basis function, edge effects due to finite-length time series and the relationship between wavelet appropriate wavelet basis function, scale and Fourier frequency (Tokgozlu et al., 2002).

If function f(t) is continuous, has null moments, decreases quickly towards zero when x tends towards infinity, or when it is null outside a segment of R, it is a likely candidate to become a wavelet. The family of shifts and dilations allows all finite energy signals to be reconstructed using the details in all scales. This property allows only continuous analysis. In the toolbox, the wavelet is usually associated with a scaling function. Wavelets, even db2, db3,..., are defined by functional equations. The solution is numerical and accomplished by using a fairly simple algorithm. A 1-D analysis is based on one scaling function and one wavelet. A 2-D analysis (on a square or rectangular grid) is based on one scaling function and three wavelets. All the functions decay quickly to zero.

In the following sections $f(t)$ will be considered as pressure height or air temperature deviations from mean values. Let $f(t)$ be a function of time and that

$$\int_{-\infty}^{\infty} |f(t)|^2 dt < \infty \tag{1a}$$

The Fourier transform F of $f(t)$ is defined as

$$F(w) = \int_{-\infty}^{\infty} f(t)e^{iwt} dt . \tag{1b}$$

A function $\psi(t)$ satisfying the following condition is called a continuous wavelet (Can et al., 2004):

$$\int_{-\infty}^{\infty} |\psi(t)|^2 dt = 1 \tag{2a}$$

and

$$\int_{-\infty}^{\infty} |\psi(t)| dt = 0 . \tag{2b}$$

Higher order moments may be zero, that is,

$$\int_{-\infty}^{\infty} t^k \psi(t) dt = 0 \quad \text{for} \quad k = 0, \ldots, N-1 .$$

2.4 Viscosity coefficients and thermal conductivity

Usually the viscosity μ_i and thermal conductivity λ_i are temperature dependent and are expressed in the following form:

$$\lambda_i = A_i T^{b_i}, \tag{3}$$

where A_i and b_i are parameters determined from fitting the experimental results. The coefficients of viscosity μ and thermal conductivity λ are computed from Dal Garno and Smith (1962):

$$\mu = 3.34 \times 10^{-7} T_o^{0.71} , \tag{4}$$

$$\lambda = 6.71 \times 10^{-4} T_o^{0.71} . \tag{5}$$

3 Analysis

3.1 Analysis of pressure heights

3.1.1 Statistical analysis

Statistical analysis of pressure height (h) with deviations at all levels is presented in Table 1. Maximum deviations (dh) are recorded at 1000 hPa, 850 hPa and 300 hPa pressure levels in winter. Maximum pressure deviations are observed at 700 hPa and 500 hPa pressure levels in spring and minimum deviations are observed at all levels in summer. Maximum annual deviations for 300 hPa, 500 hPa and 1000 hPa pressure levels are observed in 1997 and for 700 and 850 hPa in 1993.

3.1.2 Wavelet analysis

In order to illustrate the relationship between small, meso and large-scale fluctuations on air pressure and temperature, time series of five years' worth of data were analyzed by using Continuous 1-D dB-level 3 wavelet.

Large-scale effects on pressure deviations at the 850-hPa pressure level have been observed at the beginning of the first, third, fourth and fifth years (Fig. 1). Generally, the peak appears in the wavelet series of pressure disturbance in winter. Table 1 shows that amplitudes at the 500-hPa pressure level are almost two times greater than the values observed at the 850-hPa pressure level. The deviations (higher amplitudes) of pressure values at 300 hPa are higher than the deviation values recorded at lower layers.

3.2 Analysis of air temperature

3.2.1 Statistical analysis

Monthly maximum temperature deviations have been observed in spring or autumn between 1000 hPa and 300 hPa pressure levels (Table 2). If we compare the annual mean deviation values of monthly mean temperatures, the maximum values are observed between 850 and 300 hPa in 1993. For the 1000-hPa pressure level the maximum value is observed in 1994. Minimum temperature deviations, in the
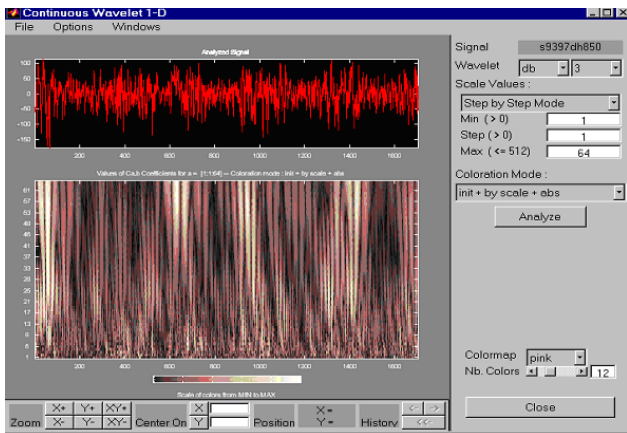
Fig. 1. Continuous wavelet 1-D analysis of the 850-hPa pressure height deviations (Istanbul, 1993–1997).
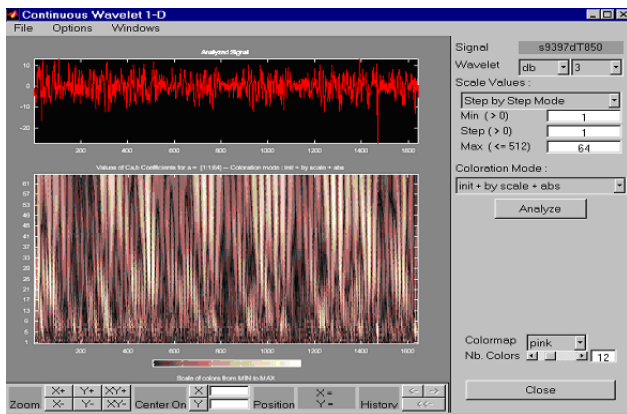

Fig. 2. Continuous wavelet 1-D analysis of air temperature deviations at the 850-hPa pressure level (Istanbul, 1993–1997).

other words weak gravity waves, have been observed between the 1000–500-hPa pressure levels in summer.

3.2.2 Wavelet analysis

Lower positive deviations have been observed at the 850-hPa pressure level (Fig. 2). Air temperature series generally show a similar pattern in this period. Their wavelet transform modulus show a main peak at the 500-hPa pressure level, in the first period of 1995. Smaller deviations between 1994 and 1996 have been recorded at the 700-hPa pressure level. Large-scale effects are more effective on dT variations at this level in the second part of the period. Generally, small-scale fluctuations play a more important role on dT values at the 500-hPa pressure level in 1993.

3.2.3 Analysis of thermal conductivity and coefficients of viscosity

Daily variations of thermal conductivity and viscosity coefficients at the 850-hPa pressure height in 1997 are analyzed (Fig. 3). Conductivity values increase at the beginning of
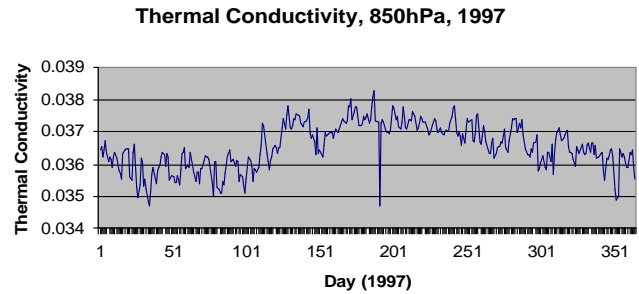

Fig. 3. Daily variation of thermal conductivity (850 hPa, 1997).

Table 3. El Niño and La Niña years in the observation period.

Year	Average SOI	Following Year	Label
1993	−1.08	1993–1994	SE (Stronger El Niño)
1994	−1.43	1994–1995	SE (Stronger El Niño)
1995	0.0	1995–1996	N (Neither)
1996	0.47	1996–1997	N (Neither)
1997	−1.67	1997–1998	SE (Stronger El Niño)

spring. They show a slightly decreasing trend in the first part of summer when energy distribution decreases.

3.3 Connections with El Niño and La Niña

Table 3 shows El Niño and La Niña years in the observation period (World Climate News, 2003).

Small standard deviation of pressure heights correspond to weak gravity waves with low amplitudes. In 1995 (neither El-Niño, nor La-Niña) the lowest amplitudes of gravity waves have been observed in summer. Strong El-Niño effects increase the amplitudes of gravity waves in summer.

Higher temperature deviations have been observed in El-Niño years (1993–1994, 1997) at the 300-, 850-, 1000-hPa pressure levels. In 1995 and 1996 (neither El-Niño nor La-Niña) lower temperature values have been observed in these pressure levels.

Large-scale effects play an important role in temperature variation. It is concluded that higher temperature and pressure deviations from mean values at lower layers (in the vicinity of 850 hPa pressure level), are observed in strong El Niño Years (1993, 1994 and 1997).

4 Results and conclusion

This is a case study which analyses daily variations of temperature and pressure deviations in the troposphere between 1993 and 1997. Wavelet analysis explains the sudden changes in parameters. It is also a useful tool for energy distribution analysis in the atmosphere.

The pressure height deviations increase above the 500-hPa pressure level in the observation period. Between 1995 and

1996 (Neutral Period: neither El-Niño nor La-Niña) the lowest deviations were observed around the 850-hPa pressure levels. Similar structures between temperature, turbulence parameters and geo-potential height deviations have been defined at all pressure levels.

References

Aslan, Z. and Oguz, O.: Time Variation of Gravity Waves in the Lower Atmosphere, IC/IR/92/22, Internal Report, 1998.

Aslan, Z., Okcu, D., and Kartal, S.: Harmonic analysis precipitation, pressure and temperature over Turkey, Il Nuovo CIMENTO, 20-4 , 595–605, 1997.

Can, Z., Aslan, Z., and Oguz, O.: The variations of temperature, pressure and wind speed values: Effects on gravity waves, Il Nuovo Cimento, 25 C, 2, 137–145, 2002.

Can, Z., Aslan, Z., and Oguz, O.: One-Dimensional Wavelet and Reanalysis of Gravity Waves, Theme Issue of the AJSE on Wavelet and Fractal Methods in Science and Engineering, Part II, 29:2C, 2004.

Dal Garno, A. and Smith, F. J.: The thermal conductivity and viscosity of atomic oxygen, Planet. Space Sci., 9, 1–6, 1962.

Ding, F., Wan, W., and Yuan, H.: The Influence of Background Winds and Attenuation on the Propagation of Atmospheric Gravity Waves, J. Atmos. Sol. Terr. Phys., 65, 857–869, 2003.

Gao, W. and Li, B. L.: Wavelet Analysis of Coherent Structures at the Atmosphere-Forest Interface, J. Appl. Meteorol., 32, 1717–1725, 1993.

Isaac, M., Renuka, G., and Venugopal, C.: Wavelet Analysis of Long Period Oscillations in Geomagnetic Field Over the Magnetic Equator, J. Atmos. Sol. Terr. Phys., 66, 919–925, 2004.

Kutiel, H., Maheras, P., Türkes, M., and Paz, S.: North Sea-Caspian Pattern (NCP) – an upper level atmospheric tele-connection affecting the eastern Mediterranean-Implications on the Regional Climate, Theoretical Applied Climatology, 72, 173–192, 2002.

Meyer, Y.: The Role of Oscillation in Some Nonlinear Problems, School on Mathematical Problems in Image Processing, ICTP, SMR1237/4, 4–22 September, 2000.

Terradellas, E., Modales, G., Cuxart, J., and Yague, C.: Wavelet Methods: Application to the Study of the Stable Atmospheric Boundary Layer Under Non-Stationary Conditions, Dyn. Atmos., 34, 2–4, 225–244, 2001.

Tokgozlu, A., Siddiqi, H., and Aslan, Z.: De Noising and Analysis of Flight Measurements, Current Trends in industrial and Applied Mathematics, edited by: Manchanda, P., Ahmad, K., and Siddiqi, A. H., Anamaya Publishers, New Delhi, 47–67, 2002.

Torrence, C. and Compo, G. P.: A Practical Guide to Wavelet Analysis, Bulletin of the American Meteorological Society, 79, 1, 61–78, 1998.

WMO: World Climate News, 23, 5, Switzerland, 2003.

Zink, F. and Vincent, R. A.: Wavelet Analysis of Stratospheric Gravity Wave Packets over Macquarie Island 1. Wave Parameters, J. Geophys. Res., 106, 10 275–10 288, 2001.